

Efficiency of 4,4'-bis(*N,N*-diethylamino) benzophenone for the polymerization of dimethacrylate resins in thick sections

Walter F Schroeder,^a Silvana L Asmussen,^a Wayne D Cook^b and Claudia I Vallo^{a*}

Abstract

The efficiency of 4,4'-bis(*N,N*-diethylamino)benzophenone (DEABP) for the polymerization of dimethacrylate monomers in thick sections (1–2 mm) was studied. DEABP ($\lambda_{\text{max}} = 365 \text{ nm}$) represents a complete initiating system as it contains both ketone and amine functional groups. During irradiation, DEABP photobleaches at a fast rate causing deeper penetration of light through the underlying layers, but the photoinitiation efficiency (rate of polymerization per photon absorption rate) is relatively poor. As a result, irradiation of methacrylate monomers at 365 nm results in a slow average polymerization rate and a reduced monomer conversion for thick sections due to the light attenuation caused by the high absorptivity of DEABP and photolysis products. These results highlight the inherent interlinking of light attenuation and photobleaching rate in polymerization of thick sections.

© 2011 Society of Chemical Industry

Keywords: frontal photopolymerization; benzophenone; dimethacrylate; photobleaching

INTRODUCTION

Light-activated dental composites are widely used in clinical restorative dentistry. Photopolymerization is commonly activated with visible light, using an initiator system comprising an α -diketone in combination with an amine reducing agent. The camphorquinone (CQ)/amine photoinitiating system is the most commonly used in current photoactivated dental materials.^{1–6} However, CQ is inherently yellow with a maximum absorbance at 470 nm,¹ which causes problems in colour matching to natural teeth. Efforts to enhance the aesthetic quality of the polymer matrix have led to the investigation of alternative photosensitizers^{7,8} which have absorption maxima at lower wavelengths. The use of UV-absorbing amino-aromatic carbonyl compounds, such as 4,4'-bis(*N,N*-dimethylamino)benzophenone (Michler's ketone), as photoinitiators has been disclosed in the patent literature,⁹ and the photochemistry of Michler's ketone has been studied by several authors.^{10–13} However, reports in the scientific literature on bulk polymerization photoinitiated with amino-aromatic carbonyl compounds are scarce.¹⁰ This encourages further research in order to assess the efficiency of these photoinitiators for the polymerization of methacrylate-based resins, in particular for the polymerization of thick sections.

4,4'-Bis(*N,N*-diethylamino)benzophenone (DEABP), a close analogue of Michler's ketone, exhibits properties that make it attractive as a photoinitiator of dental composites. DEABP represents a complete initiating system as its molecule contains both ketone and amine functional groups and it exhibits a strong absorption at 365 nm but does not absorb significantly in the visible region and so is more neutral in colour compared with CQ. An additional reason for investigating the use of DEABP as a dental photoinitiator is motivated by the current availability on the market of curing

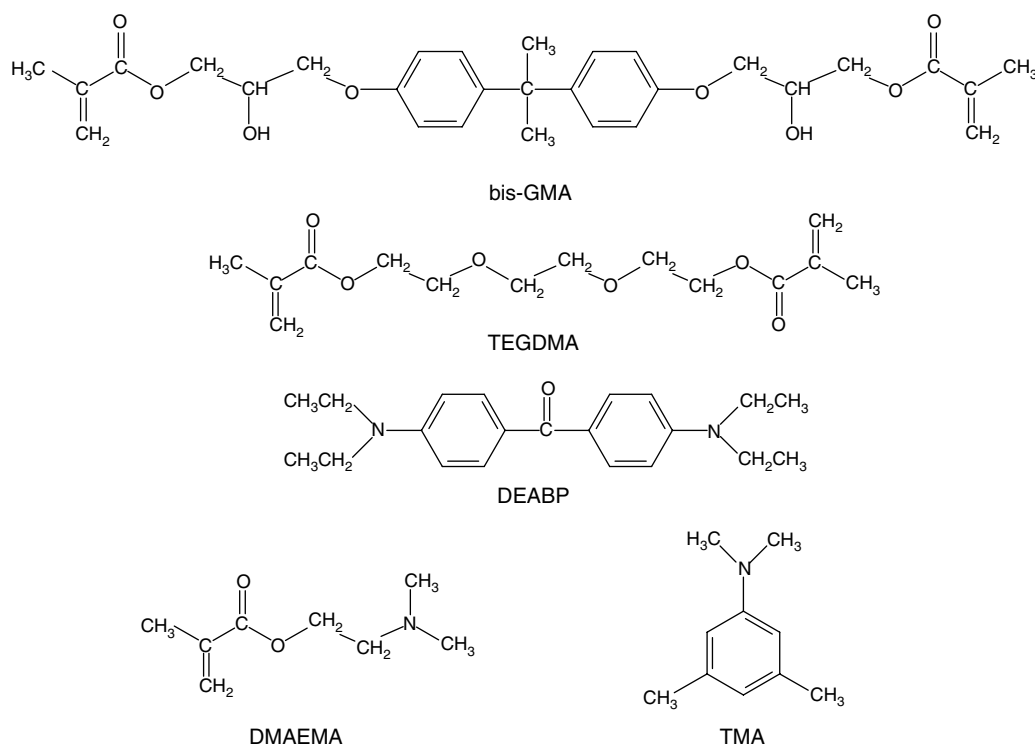
radiation sources of light-emitting diode (LED) technology which can emit narrow-band radiation centred at wavelengths ranging from approximately 350 to 500 nm, thus potentially overlapping with the spectrum of DEABP.

Photopolymerization of thick systems (*ca* 1–2 mm) is less common than radiation-induced polymerization of thin films and coatings (*ca* 20–100 μm). This can be attributed to the reduced cure rate and depth of cure caused by the effect of the initiator absorptivity on the optical attenuation of the radiation with increasing sample thickness. On the other hand, in many photoinitiation systems, the photoinitiator is photobleached during the irradiation, producing moieties which are transparent or have lower absorption coefficients at the wavelength of interest. Because the absorbing photoinitiator is destroyed upon radiation exposure, the incident radiation progressively penetrates deeper into thick samples.^{14–19} Thus, the study of photobleaching characteristics of photoinitiators used for the polymerization of thick layers, as is the case for dental restorative resins, is an essential step for a proper understanding of the photopolymerization process.

* Correspondence to: Claudia I Vallo, Institute of Materials Science and Technology (INTEMA), Universidad Nacional de Mar del Plata-National Research Council (CONICET), Av. Juan B Justo 4302, 7600 Mar del Plata, Argentina. E-mail: civallo@fi.mdp.edu.ar

a Institute of Materials Science and Technology (INTEMA), Universidad Nacional de Mar del Plata–National Research Council (CONICET), Av. Juan B Justo 4302, 7600 Mar del Plata, Argentina

b Department of Materials Engineering, Monash University, Melbourne, Victoria 3800, Australia



Scheme 1. Structure of the monomers and photoinitiator systems studied.

The purpose of the study reported here was to examine the suitability of DEABP for the polymerization of dimethacrylate-based dental resins in thick (2 mm) samples. The photodecomposition of DEABP was studied in both organic solvents and dimethacrylate monomers. The efficiency of DEABP was assessed by monitoring the progress of monomer conversion *versus* irradiation time. Results obtained are explained in terms of the inherent interlinking of light attenuation and photobleaching rate in bulk polymerizing systems.

EXPERIMENTAL

Materials

The resins were formulated from blends of 2,2-bis[4-(2-hydroxy-3-methacryloxyprop-1-oxy)phenyl]propane (bis-GMA; Esstech, Essington, PA) and triethylene glycol dimethacrylate (TEGDMA; Aldrich) at mass fraction of 70:30. Bis-GMA and TEGDMA were used as received. The 70:30 bis-GMA/TEGDMA blend is denoted BisTEG. The resins were activated for UV light polymerization by the addition of DEABP (Aldrich). CQ (Aldrich) was used as a comparison photoinitiator in combination with *N,N*-3,5-tetramethylaniline (TMA; Aldrich) and dimethylamino ethylmethacrylate (DMAEMA; Aldrich) which act as reducing agents. The solvents acetonitrile (Merck) and ethanol (Merck) and the above-mentioned materials were employed as received. The structures of the monomers and photoinitiator systems are depicted in Scheme 1.

Radiation source

The radiation source was assembled from an LED with its irradiance centred at 365 nm (OTLH-0480, Optotech Inc.). The LED was selected taking into account that DEABP has its absorption peak also near 365 nm. The intensity of the LED was measured with the chemical actinometer potassium ferrioxalate, which is

recommended for the 253–577 nm wavelength range.²⁰ The irradiance of the LED, I_0 , was set at three different values by varying the electrical voltage through the semiconductor: 85, 135 and 175 mW cm⁻².

Photolysis of DEABP

The photodecomposition of DEABP was followed using the changes in absorbance at the wavelength of its maximum absorption. The absorption spectra of DEABP were measured with a UV-visible spectrophotometer (1601 PC, Shimadzu) at room temperature (*ca* 20 °C) in acetonitrile, ethanol and BisTEG resins, using identical cells but containing only the solvent or monomer as a reference. Bleaching experiments in acetonitrile and ethanol were carried out in 1 mm thick quartz cuvettes under nitrogen or air atmosphere. Solutions of DEABP in acetonitrile and ethanol were de-aerated by bubbling with nitrogen for about 20 min before irradiation. The concentration of DEABP in acetonitrile or ethanol was 2×10^{-4} mol L⁻¹ (0.006 wt%). Photodecomposition studies with the BisTEG resins in an air environment were carried out in 2.0 ± 0.2 mm thick samples sandwiched between two disposable 1 mm thick glass plates. The concentration of DEABP in BisTEG resin was 7.1×10^{-5} mol L⁻¹ (0.002 wt%). The molar absorption coefficient of DEABP was 49 570 L mol⁻¹ cm⁻¹ in acetonitrile, 45 820 L mol⁻¹ cm⁻¹ in ethanol and 37 260 L mol⁻¹ cm⁻¹ in methacrylate resin. The absorbance of a 2 mm thick sample of the methacrylate resin at 365 nm was 0.027. The samples were irradiated at 85, 135 or 175 mW cm⁻².

Measurement of double bond conversion

Fourier transform infrared (FTIR) spectra were acquired with a Nicolet 6700 Thermo Scientific. Near-infrared (NIR) spectra were acquired over the range 4500–7000 cm⁻¹ from 16 co-added scans

at 2 cm^{-1} resolution. The resins were sandwiched between two glass plates separated by a 2 mm rectangular rubber spacer and were tightly attached to the sample holder using small clamps. With the assembly in a vertical position, the radiation source (175 mW cm^{-2}) was placed in contact with the glass surface. The specimens were irradiated at regular time intervals and spectra were collected immediately after each exposure interval. The background spectra were collected through an empty mould assembly fitted with only one glass slide to avoid internal reflectance patterns. The conversion profiles were calculated from the decay of the absorption band^{5,21} located at 6165 cm^{-1} . The concentration of DEABP in BisTEG resin was $1.79 \times 10^{-3}\text{ mol L}^{-1}$ (0.05 wt%).

As a comparison with the photocuring behaviour of DEABP, the conversion in a BisTEG resin containing 1 wt% (0.07 mol L^{-1}) CQ in combination with an equimolar proportion of TMA was measured from NIR spectra. This resin was irradiated with a 470 nm LED (the absorbance maximum of CQ) at 30 mW cm^{-2} irradiance. Two replicates of each of the resins were used in the measurement of conversion.

The relative photocuring efficiency of DEABP and CQ was also evaluated for $ca\ 20\ \mu\text{m}$ films of BisTEG contained between pressed KBr discs using mid-FTIR spectra with the methacrylate absorption band located at 1637 cm^{-1} . For this study, the BisTEG resin was formulated with either DEABP or equimolar CQ/TMA at a concentration such that there was minimal attenuation of the radiation through the film and so that both had similar amounts of absorbed radiation (ϵCl , which can be expressed in moles of photons absorbed per second per unit volume). This was achieved by comparison of a resin formulation containing $1.5 \times 10^{-3}\text{ mol L}^{-1}$ DEABP irradiated with 1.75 mW cm^{-2} at 365 nm ($5 \times 10^{-9}\text{ einstein cm}^{-2}$) with a resin containing 0.07 mol L^{-1} CQ irradiated with 175 mW cm^{-2} at 470 nm ($10^{-7}\text{ einstein cm}^{-2}$). In this way, the efficiency of DEABP and CQ/TMA could be compared in terms of the relative rates of polymerization per mole of photons absorbed per unit time in a unit volume.

RESULTS AND DISCUSSION

Photolysis of DEABP in various solvents

The mechanism of photodecomposition of ketone/amine systems has been reported in previous research,^{1–4,10} and specifically for Michler's ketone.¹³ By analogy to the latter, the photolysis of DEABP results in the following radicals:¹³

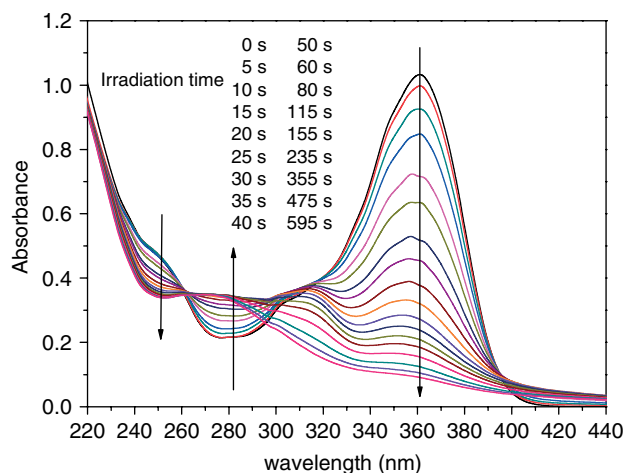
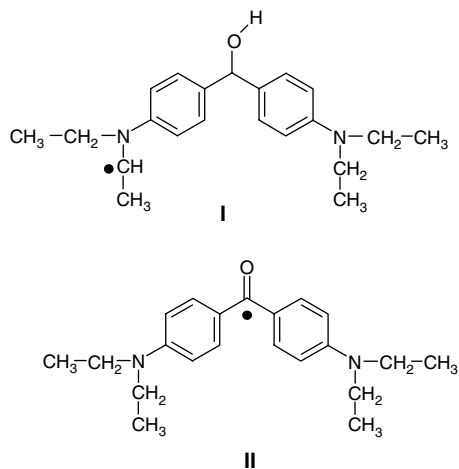


Figure 1. Typical spectral changes during the irradiation of a $2 \times 10^{-4}\text{ mol L}^{-1}$ solution of DEABP in acetonitrile under air in a 1 mm thick cuvette. $I_0 = 175\text{ mW cm}^{-2}$.

It is generally accepted that upon absorption of light the carbonyl group is promoted to an excited singlet state.^{1–4} This excited state may return to the ground state or it may decompose into another species. The excited singlet may also undergo intersystem crossing to the triplet state. The excited triplet then forms an exciplex with a ground-state DEABP molecule via electron donation by the amine to the carbonyl, thus producing two radical ions. In some cases, this charge transfer complex may be deactivated to the starting species or may form a degradation product. However, if proton abstraction occurs, then two neutral free radicals are formed. For related ketone/amine photoinitiation systems^{1–5} it is generally considered that the amine radical is responsible for initiating the polymerization and that the radical formed from the ketone is not an efficient initiator due to a steric hindrance effect and because it dimerizes.^{1–5} Alternatively, hydrogen abstraction from another suitable donor, such as monomer, by the excited triplet may result in ketyl and donor-derived radicals.

Since the initiator decomposition can involve interaction with the chemistry of the matrix, the photodecomposition of DEABP photoinitiator was studied in acetonitrile, ethanol and BisTEG by monitoring the decrease in absorbance at the wavelength of the maximum absorption of DEABP. Figure 1 shows that the band near 365 nm decreases monotonically with irradiation time and the consumption of DEABP is accompanied by the appearance of UV-absorbing photoproducts (illustrated by the increased absorbance of the band at 275 nm). Similar trends are observed during irradiation of DEABP in either ethanol (not shown here) or methacrylate monomer (Fig. 2), but the photolysis process was slower and faster, respectively.

Irradiation of DEABP in BisTEG (Fig. 2) results in almost complete photobleaching after several seconds of irradiation. Hydrogen abstractions from another DEABP molecule and from monomer structures are competitively involved in the photoreduction of DEABP. The TEGDMA monomer contains ether methylene groups which may serve as a source of abstractable hydrogens. The absorbance of the photoproduct was assessed by irradiating BisTEG resin samples containing various concentrations of DEABP until a constant value of absorbance was reached. The final absorbance associated with the presence of absorbing photoproducts is an approximately linear function of the initial concentration of DEABP which indicates that the photolysis

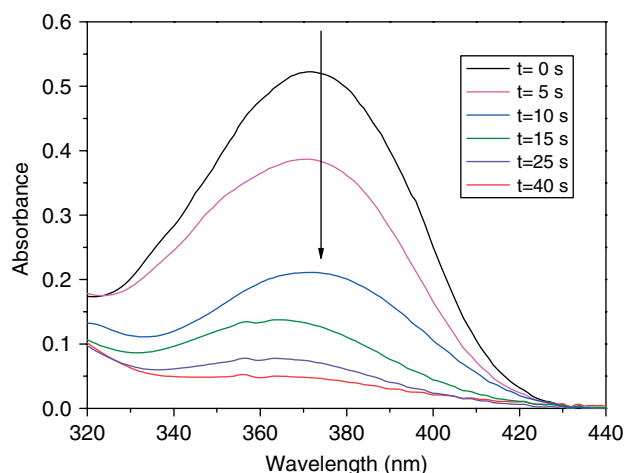


Figure 2. Typical spectral changes during the irradiation of a $7.1 \times 10^{-5} \text{ mol L}^{-1}$ solution of DEABP in BisTEG resin saturated with air in a 2 mm thick specimen. $I_0 = 175 \text{ mW cm}^{-2}$.

of DEABP involves a process of the form $A \rightarrow B$, where A (DEABP) absorbs more strongly than B (the photolysis product of DEABP). From the relationship between the increase in absorbance due to the appearance of the photoproduct and the decrease in absorbance due to the photobleaching of the DEABP, the absorption of the sample at 365 nm can be predicted.

As an approximation, the maximum absorbance at 365 nm for the data shown in Fig. 2 was fitted to an exponential decay, to test the assumption that the rate of photolysis is first order with respect to the DEABP concentration. Analysis of these data shows that the DEABP concentration decays exponentially with a decay constant of $0.090 \pm 0.002 \text{ s}^{-1}$ (R^2 correlation coefficients of 0.98) as expected of a first-order dependence of the rate on DEABP concentration. This analysis is an approximation because the radiation intensity decreases by as much as 70% through the sample due to the screening effect of the photoinitiator. To accurately analyse photolysis data such as those shown in Figs 1 and 2, the photolysis rate of the photoinitiator at a particular depth needs to be determined and integrated over the thickness of the specimen. When this is done, the average rate of decomposition of DEABP is related to the quantum yield and the radiation absorbed (I_{abs}) by the expression^{14,22}

$$-\frac{dC}{dt} = \frac{\Phi I_{\text{abs}}}{L} = \frac{\Phi I_0 (1 - e^{-\alpha C L})}{L} \quad (1)$$

Here, C is the average concentration of DEABP, Φ is the quantum yield of DEABP consumption (the fraction of DEABP molecules decomposed per photon absorbed), I_0 is the incident irradiance (in moles of photons per unit time per unit area), L is the sample thickness and α is the Napierian absorption coefficient (i.e. the molar absorption coefficient multiplied by 2.303). For simplicity (but not by necessity), in Eqn (1) we assume here that the rate of photolysis is proportional to the radiation intensity; this is confirmed by experimental studies as discussed below. Integrating Eqn (1) yields

$$\ln \left(\frac{10^{\alpha C L} - 1}{10^{\alpha C_0 L} - 1} \right) = \ln \left(\frac{10^A - 1}{10^{A_0} - 1} \right) = -\alpha \Phi I_0 t \quad (2)$$

where C_0 is the initial DEABP concentration, the absorbance of the sample, A , is equal to $(\alpha C L)$ and the term $(\alpha \Phi I_0)$ is the pseudo-first-

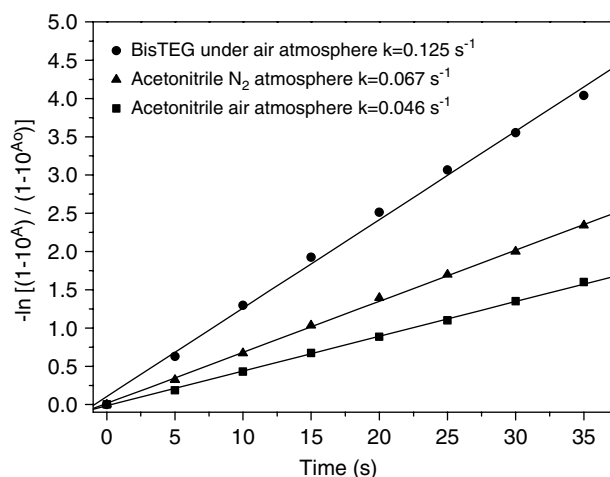


Figure 3. Plots of Eqn (2) at a wavelength of 365 nm for solutions of DEABP in various media. $I_0 = 175 \text{ mW cm}^{-2}$. Parameter $k = \Phi \alpha I_0$ is the constant rate for photobleaching of DEABP.

Table 1. Rate constant^a for photobleaching of DEABP for various irradiances and media

Solvent ^b	Irradiance (mW cm ⁻²)	k in air (s ⁻¹)	k in nitrogen (s ⁻¹)
Acetonitrile	85	0.0179 (± 0.002)	0.0328 (± 0.003)
Acetonitrile	135	0.0310 (± 0.003)	0.0495 (± 0.002)
Acetonitrile	175	0.0460 (± 0.002)	0.0670 (± 0.005)
Ethanol	135	1.8×10^{-4} (± 0.00006)	4.3×10^{-4} (± 0.00004)
BisTEG	175	-	
		0.125 (± 0.003)	

^a Rate constant $k = \Phi \alpha I_0$.
^b Concentration of DEABP in ethanol and acetonitrile was $2 \times 10^{-4} \text{ mol L}^{-1}$ and was $7.1 \times 10^{-5} \text{ mol L}^{-1}$ in BisTEG resin.

order rate constant (k) for the photobleaching of DEABP. Thus, using the wavelength of 365 nm, a plot of Eqn (2) should give a straight line whose slope is proportional to the rate constant for the DEABP consumption. In order to minimize interferences due to light absorption by the photoproduct, only the absorbance values ranging from 100 to 5% of the initial absorbance were used to calculate the rate constant of photolysis in various solvents. Plots of Eqn (2) are depicted in Fig. 3. The good linear fit of Eqn (2) (Fig. 3) demonstrates that the assumption of first-order kinetics for the decomposition of DEABP is satisfactory. The photodecomposition of CQ/amine pairs was studied by Cook¹ who reported a first-order expression for CQ loss. The analysis of the kinetic scheme for the photoinduced consumption of CQ proposed by that author¹ reveals that first-order behaviour is observed when the intersystem crossing from the excited singlet state to the triplet state is the rate-determining step.

Measurements of the photobleaching of DEABP under nitrogen or air can reveal the importance of triplet state quenching of the excited state by oxygen. Table 1 shows that the constant rate (k) for the photobleaching DEABP is lower under an air atmosphere than under nitrogen, indicating that the quenching of the triplet state of DEABP by dissolved oxygen is significant and so reduces

the rate of loss of DEABP. Also shown by the data in Table 1, the rate of photobleaching of DEABP depends on the solvent used – the reason for this is unclear but presumably depends on the relative efficiency of the reactions involved in the photodecomposition of DEABP.¹³

Table 1 also indicates that the effect of increased radiation intensity decreases the time constant and increases the rate of photobleaching. Least-squares fitting of these limited data gives R^2 correlation coefficients in excess of 0.98, indicating that the assumption of a first-order dependence of photobleaching rate on radiation intensity is valid.

The rate of photolysis of DEABP in BisTEG does not appear to be significantly affected by the changes in the resin as a result of gelation by vitrification. This is in agreement with results reported on photobleaching of CQ in methacrylate resins.^{23,24} The photoinduced self-redox reaction between the ketone and amine groups of two DEABP molecules depends on the excitation of the DEABP to the singlet state and then its conversion to a triplet state, the diffusion of the reactants, the mutual reorientation and multiple collision of the reactants and the dissociation of the transition state to give the final radicals. Of these, the diffusional steps should be highly dependent on the viscosity or rigidity of the medium. However, an analysis of the kinetic scheme for the photoinduced consumption of CQ proposed by Cook¹ reveals that a the rate of photolysis will be independent of molecular mobility if the intersystem crossing from the excited singlet state to the triplet state is the rate-determining step, as discussed above.

Double bond conversion versus irradiation time

Photopolymerization experiments were carried out in the presence of oxygen in order to simulate practical applications of the photoinitiator. It is worth mentioning, however, that oxygen inhibition is known to be one of the major problems in light-induced free radical polymerization. Three inhibition mechanisms involving oxygen in photoinduced radical polymerization are: quenching of the photoinitiator triplet state, reaction with primary radicals or reaction with propagating radicals.^{2,4,25} Photoinitiating systems which involve tertiary aliphatic amines can be useful in suppressing inhibition by the reaction of oxygen with the C-based radicals through the radical chain transfer process which regenerates the initiation reaction:⁴



The radical, R^{\bullet} , in Eqn (4) may be an amine or monomer radical.⁴

The progress of monomer conversion versus irradiation time was studied in BisTEG resin containing $1.79 \times 10^{-3} \text{ mol L}^{-1}$ (0.05 wt%) of DEABP and an irradiance of 175 mW cm^{-2} . This concentration was selected from exploratory measurements of conversion versus time which balanced the effects of undercure and attenuation of the radiation at depth. At DEABP concentrations much lower than 0.05 wt%, the 2 mm thick samples studied are only partially cured after 200 s irradiation, after which the reaction is effectively terminated, presumably due to consumption of DEABP and then of radicals by the action of residual oxygen or inhibitor in the resin. On the other hand, at DEABP concentrations much higher than 0.05 wt%, the attenuation of the radiation by DEABP absorption limits the depth of cure. As an example, a 2 mm thick sample containing 0.5 wt% DEABP and irradiated for more than 600 s contains non-polymerized resin on the far side of the sample

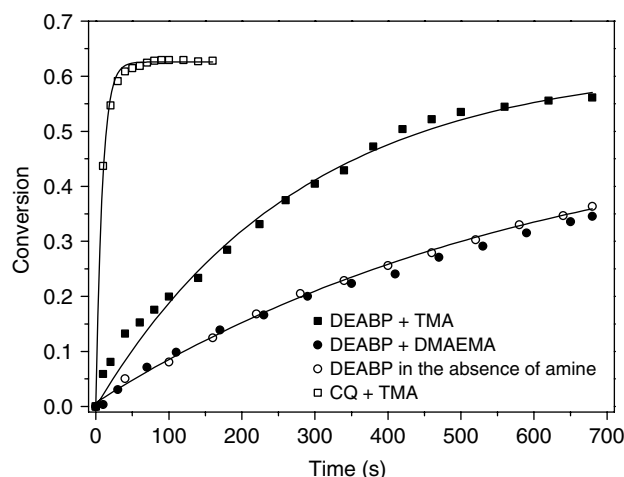


Figure 4. Global conversion (measured using NIR spectra) versus irradiation time for a 2 mm thick BisTEG resin specimen containing $1.79 \times 10^{-3} \text{ mol L}^{-1}$ DEABP in the absence of amine and in combination with 0.07 mol L^{-1} of either TMA or DMAEMA. $I_0 = 175 \text{ mW cm}^{-2}$. Conversion of a resin containing 0.07 mol L^{-1} (1 wt%) CQ/MA irradiated with a 470 nm LED of $I_0 = 30 \text{ mW cm}^{-2}$ is shown for comparison.

holder which does not cure until after 20 min of exposure. Thus, the concentration of DEABP used in conversion measurements was selected from a compromise between minimizing the irradiation time and maximizing the monomer conversion. Figure 4 shows the global conversion (i.e. the average conversion through the sample thickness) versus irradiation time of the resin containing 0.05 wt% DEABP. Conversions of formulations containing 0.05 wt% DEABP in combination with $7 \times 10^{-2} \text{ mol L}^{-1}$ of DMAEMA or TMA are also shown in Fig. 4.

As discussed above, in polymerization reactions photoinitiated by ketone/amine systems, the amine radical is responsible for initiating the polymerization.^{1–4} Although the radicals produced by the photodecomposition of DEABP are found to induce polymerization, the monomer conversion progresses at a slow rate (Fig. 4). No significant improvement in the rate of monomer conversion is observed by the combination of DEABP with the aliphatic amine DMAEMA; however, combination with a good hydrogen donor, such as the aromatic amine TMA,^{1,5} significantly increases the cure rate. This observation is in agreement with previous studies on CQ/amine as photoinitiation pairs.^{1,5}

DEABP has a higher molar absorptivity and higher rate of bleaching compared with CQ/amine photoinitiator systems traditionally used in dentistry. The molar absorption of CQ in BisTEG resin is $42 \text{ L mol}^{-1} \text{ cm}^{-1}$ at 470 nm and the rate constant of photobleaching is 0.045 s^{-1} at 175 mW cm^{-2} ,^{23,24} while the molar absorption of DEABP in BisTEG resin is $37\,260 \text{ L mol}^{-1} \text{ cm}^{-1}$ at 365 nm and the rate constant of photobleaching is 0.125 s^{-1} at 175 mW cm^{-2} . The lower polymerization rate observed for photoinitiation by DEABP in comparison to CQ/TMA (Fig. 4) may be attributed to both the lower reactivity of DEABP and the filtering or screening effect caused by the high value of the absorption coefficient of DEABP compared with CQ. To determine the validity of these factors, mid-FTIR photocuring studies were performed on ca 20 μm samples having similar absorbed radiation dose rates. The conversion in BisTEG activated with 0.07 mol L^{-1} CQ and irradiated with $10^{-7} \text{ einstein cm}^{-2}$ at 470 nm for 100 s is 60% higher than that reached in resins containing $0.0015 \text{ mol L}^{-1}$ DEABP irradiated with $5 \times 10^{-9} \text{ einstein cm}^{-2}$ at 365 nm. It is worth noting that in order

to minimize attenuation effects, the concentration of DEABP must be low. Under that condition, it is conceivable that a significant fraction of the DEABP radicals are consumed by inhibitor and oxygen in the resin. The overall effect of light screening on the polymerization of thick sections is a reduced photoinitiation rate and consequently a reduced double bond conversion along the irradiation path. The combined effects of light attenuation and photobleaching rate on the photoinitiation rate as a function of depth into the sample are analysed below.

Evolution of photoinitiation rate versus time and depth

The evolution of photoinitiator concentration and photoinitiation rate as a function of time and depth into the sample can be computed from the coupled system of equations which describe the photoinitiator decomposition rate (Eqn (5)) and radiation attenuation according to the Beer–Lambert law (Eqn (6)). The variation of the photoinitiator concentration with irradiation time is given by^{14,22}

$$-\frac{\partial C(x, t)}{\partial t} = \Phi \alpha I(x, t) C(x, t) \quad (5)$$

where x is the depth through the sample thickness (at the irradiated surface $x = 0$, while $x = L$ where the radiation exits the sample) and $C(x, t)$ and $I(x, t)$ are the photoinitiator concentration and light intensity, respectively, which are functions of time and position along the sample thickness. The irradiance at a particular depth, $I(x, t)$, decreases with sample thickness according to the integrated form of the Beer–Lambert law:

$$I(x, t) = I_0 \exp \left[- \sum_{i=1}^N \alpha_i \int_0^L C_i(x, t) dx \right] \quad (6)$$

where α_i and C_i are the Napierian absorption coefficient and concentration of the i th absorbing species, of which there are N .

If only the photoinitiator absorbs, i.e. the initiator fragments and the monomer are both non-absorbing, then Eqns (5) and (6) can be solved analytically^{14–16} and the concentration of photoinitiator (C), light intensity (I) and photoinitiation rate (R_i , equal to the product of the concentration, intensity and quantum yield) as a function of time and depth are given by the following equations (symbols used in Eqns (7)–(9) are listed in Table 2):

$$\frac{C(z, t)}{C_0} = \frac{1}{1 - e^{-\gamma z} (1 - e^{kt})} \quad (7)$$

$$\frac{I(z, t)}{I_0} = \frac{e^{(kt - \gamma z)}}{1 - e^{-\gamma z} (1 - e^{kt})} \quad (8)$$

$$R_i(z, t) = \frac{e^{(kt - \gamma z)}}{[1 - e^{-\gamma z} (1 - e^{kt})]^2} \quad (9)$$

For the generalized case, which includes the effects of absorption by the initiator fragments and absorption by the monomer, the coupled differential Eqns (5) and (6) can only be solved using a numerical approach. As described in the photolysis studies, the final absorbance associated with the presence of absorbing photoproducts in the BisTEG resin (A_p) is a linear function of the initial absorbance of the DEABP (A_i). From the known relationship between the increase in absorbance due to the appearance of the photoproducts and the decrease in absorbance due to the photobleaching of the DEABP ($A_p = 0.11A_i$),

Table 2. Symbols used in equations

Symbol	Description	Units
x	Layer depth or position in layer	m
L	Layer thickness	m
$z = x/L$	Dimensionless coordinate	
C	Concentration of DEABP	mol L ⁻¹
Φ	Quantum yield of DEABP consumption	
ε	Absorption coefficient of DEABP	L mol ⁻¹ cm ⁻¹
$\alpha = 2.303\varepsilon$	Nepierian absorption coefficient of DEABP	L mol ⁻¹ cm ⁻¹
I_0	Incident light irradiance	mW cm ⁻²
$k = \Phi \alpha I_0$	Rate constant for photobleaching of DEABP	s ⁻¹
$\gamma = \alpha C_0 L$	Initial absorbance	

Eqns (7)–(9) are solved by the method of finite differences to give the spatiotemporal distribution of photoinitiator concentration, light intensity and photoinitiation rate. Time and depth increments equal to 0.005 s and 0.005 mm are used. To verify the accuracy of the numerical method, the numerical solution (Eqns (7)–(9)) is compared to the analytical solution (Eqns (5) and (6)) for the case of no absorption by the initiator fragments – for the mesh sizes used, the two methods give essentially identical results. Computations are made for a 2 mm thick section containing 1.79×10^{-3} mol L⁻¹ (0.05 wt%) DEABP, the absorbance of the monomer is 0.027 and $I_0 = 175$ mW cm⁻². The effect of perfect bleaching predicted by the analytic solution in Eqns (5) and (6) is also calculated in order to assess the effect of the absorptivity of the photolysis product on the gradients of photoinitiation rate.

Figure 5(a) shows the light intensity as a function of time and depth assuming perfect bleaching. The light intensity at the exposed surface is equal to the incident light intensity at all times. Due to the high molar absorptivity of DEABP the radiation is drastically attenuated through the sample thickness. However, upon irradiation, the absorbing photoinitiator is destroyed, and therefore the radiation progressively penetrates deeper into the sample. For this perfect bleaching system, the light intensity at a depth $x = 1$ mm reaches that of the incident light (at $x = 0$) after 150 s exposure. Conversely, if one allows for the production of light-absorbing photolysis compounds, the light intensity in the deeper layers of the sample never reaches the value of the incident light because the absorbing species nearest to the light source absorb part of it. Since the production of light-absorbing compounds increases with irradiation time, the light intensity that reaches the deeper layers decreases. This effect is illustrated in Fig. 5(b), which shows that the maximum value of light intensity that reaches a depth $x = 1$ mm is about 40% of the incident light intensity.

Figures 6(a) and (b) show the concentration profiles of DEABP within the sample, and how they move progressively inside with exposure time. Initially, the initiator concentration is uniform, and the light intensity decreases with depth according to the Beer–Lambert law. Immediately after irradiation commences, the initiator is consumed at a rate proportional to the local light intensity (Eqn (5)), thereby leading to an initiator concentration gradient along the beam direction. For a perfect bleaching system (Fig. 6(a)), DEABP is completely consumed for depths $x \leq 0.5$ mm

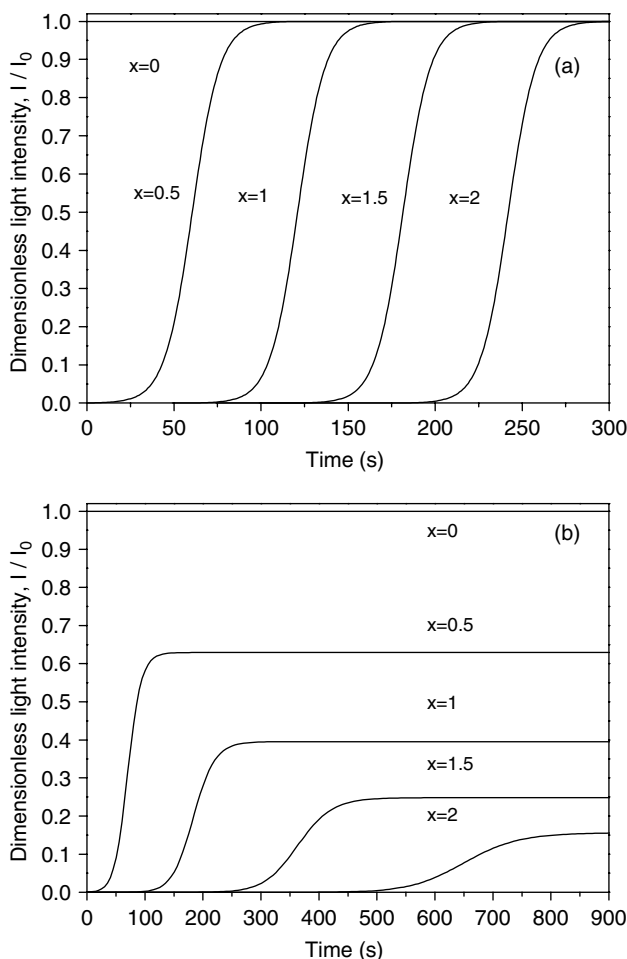


Figure 5. (a) Time and depth dependence of the normalized light intensity in a 2 mm thick sample calculated for perfect bleaching from Eqn (8). $I_0 = 175 \text{ mW cm}^{-2}$, $C_0 = 1.79 \times 10^{-3} \text{ mol L}^{-1}$ (0.05 wt%), $\gamma = 30.5$, $k = 0.125 \text{ s}^{-1}$. (b) As (a) taking into account that an absorbing product is formed. The absorbance of the photoproduct is 0.11 times the initial absorbance of DEABP. Note the difference in abscissa scale compared with (a).

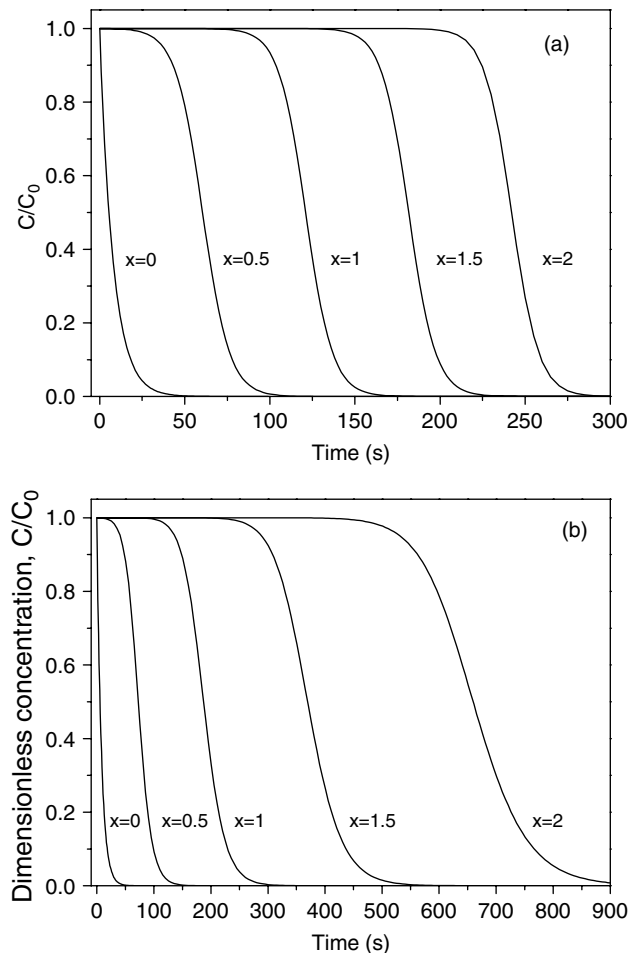


Figure 6. (a) Dimensionless initiator concentration versus time and depth in a 2 mm thick sample calculated for perfect bleaching from Eqn (7). $I_0 = 175 \text{ mW cm}^{-2}$, $C_0 = 1.79 \times 10^{-3} \text{ mol L}^{-1}$ (0.05 wt%), $\gamma = 30.5$, $k = 0.125 \text{ s}^{-1}$. (b) As (a) taking into account that an absorbing product is formed. The absorbance of the product formed is 0.11 times the absorbance of the DEABP consumed. Note the difference in abscissa scale compared with (a).

after about 100 s exposure whereas no significant consumption occurs at $x \geq 1 \text{ mm}$. After 150 s exposure, little initiator remains in the front half ($x \leq 1$) of the layer, while little has been consumed in the rear half ($x \geq 1 \text{ mm}$). For a given exposure time, the photoinitiator concentration profile has a large and almost constant gradient as a function of the thickness. Figure 6(b) shows the concentration profiles of DEABP calculated taking into account the presence of photoproducts. As a result of the production of light-absorbing photolysis compounds, the light intensity that reaches the deeper layers decreases, thereby reducing the rate of consumption of DEABP. In this case, for a given exposure time, the photoinitiator concentration profile has a smaller and decreasing gradient as a function of thickness.

Figure 7 shows that the spatiotemporal variation of the photoinitiation rate is highly localized. The wavelike behaviour is attributed to the fact that the local photoinitiation rate is proportional to the product of photoinitiator concentration and light intensity which varies in an inverse but slightly out-of-phase manner as a function of depth. This kind of photoinitiated polymerization, propagating through the whole thickness, has been defined as photoinitiated frontal polymerization.^{14–19,26,27}

For a perfect bleaching system, the waveform propagates downbeam and the peak exits the layer at 300 s. Consequently, after 300 s irradiation, the initiation rate along the sample thickness is effectively zero due to the consumption of DEABP. Figure 7(b) illustrates the effect of the presence of absorbing photolysis product on the photoinitiation rate for the same conditions shown in Fig. 7(a). As the photoinitiator is consumed, part of the incident light intensity is absorbed by the photoproducts and, consequently, the photoinitiation rate decreases with depth.

The presence of absorbing photoproducts reduces the light penetration into the resin and consequently the speed of propagation of the photoinitiation rate waves (Fig. 7(b)). Therefore, it is difficult to achieve thick-section cure for a non-perfect bleaching photoinitiator, and this effect is magnified as the initiator concentration or sample thickness is increased.

CONCLUSIONS

The efficiency of DEABP for the polymerization of methacrylate monomers in thin and thick sections was assessed. Although the radicals produced by the photodecomposition of DEABP

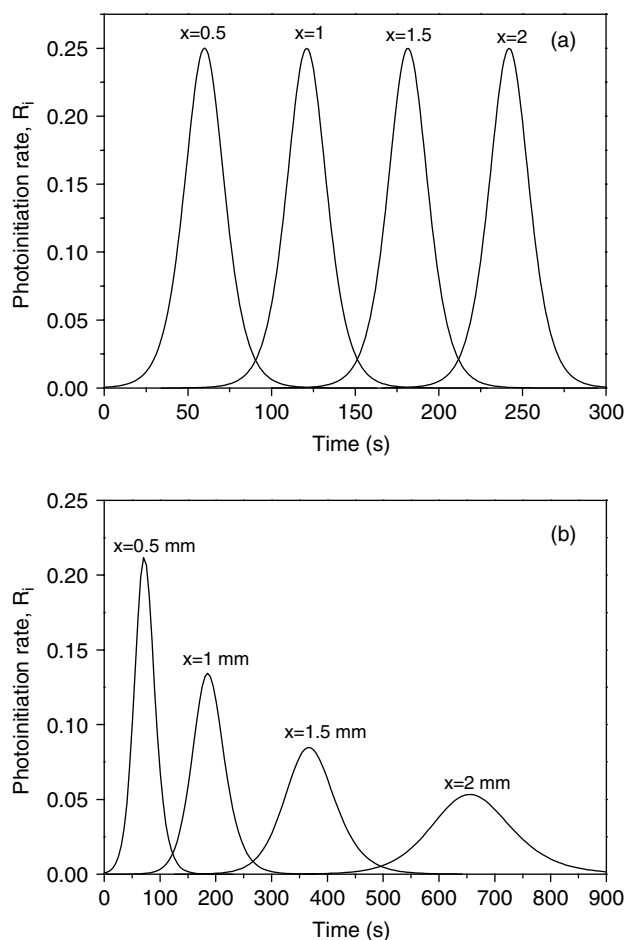


Figure 7. (a) Time and depth dependence of the photoinitiation rate in a 2 mm thick sample. $I_0 = 175 \text{ mW cm}^{-2}$, $C_0 = 1.79 \times 10^{-3} \text{ mol L}^{-1}$ (0.05 wt%), $\gamma = 30.5$, $k = 0.125 \text{ s}^{-1}$. (b) As (a) taking into account that an absorbing product is formed. The absorbance of the photoproduct is 0.11 times the initial absorbance of the DEABP. Note the difference in abscissa scale compared with (a).

induced polymerization, the monomer conversion progressed at a relatively slow rate, especially for thick sections. Results obtained in the present study highlight the inherent interlinking of light attenuation, photobleaching rate and presence of absorbing photolysis compounds in bulk polymerizing systems. Radiation attenuation and photoinitiator consumption compete to determine the local initiator concentration and light intensity distribution, and hence the local initiation rate. The evaluation of a photoinitiator to be used for the polymerization of dental resins is governed by the requirement of a high curing speed so that the polymerization is complete in a short time (*ca* 60 s). DEABP has a high molar absorptivity and higher rate of bleaching compared with traditional CQ/amine photoinitiator

systems. However, the presence of absorbing photoproducts attenuates drastically the light in the sample. In order to enhance the advance of the photoinitiation front, low concentrations of DEABP are required. Unfortunately, this results in limited degree of monomer conversion due to depletion of the radicals by residual oxygen or inhibitors. From the results presented it emerges that DEABP is not an efficient photoinitiator for the polymerization of thick sections when rapid cure is required, as is the case for dental applications.

ACKNOWLEDGEMENTS

The financial support provided by the ANPCyT PICT00550 and by the ARC DP1093217 is gratefully acknowledged. The authors are grateful to Esstech for the donation of the Bis-GMA monomer.

REFERENCES

- 1 Cook WD, *Polymer* **33**:600 (1992).
- 2 Jakubiak J, Allonas X, Fouassier JP, Sionkowska A, Andrzejewska E, Linden LA, *et al*, *Polymer* **44**:5219 (2003).
- 3 Nie J, Linden LA, Rabek JF, Fouassier JP, Morlet-Savary F, Scigalski F, *et al*, *Acta Polym* **49**:145 (1998).
- 4 Nie J, Andrzejewska E, Rabek JF, Linden LA, Fouassier JP, Paczkowski J, *et al*, *Macromol Chem Phys* **200**:1692 (1999).
- 5 Schroeder W and Vallo C, *Dent Mater* **23**:1313 (2007).
- 6 Hongguang X, Gangqiang W and Nie J, *J Photochem Photobiol A* **193**:254 (2008).
- 7 Schroeder W, Arenas G and Vallo CI, *Polym Int* **56**:1099 (2007).
- 8 Asmussen S and Vallo CI, *J Photochem Photobiol A* **202**:228 (2009).
- 9 Giangualano MN, US Patent 33761369 (1968).
- 10 McGinniss VD, Provder T, Kuo C and Gallopo A, *Macromolecules* **11**:393 (1978).
- 11 Schuster DI, Goldstein MD and Bane P, *J Am Chem Soc* **99**:187 (1977).
- 12 Bamabas MV, Liu A, Trifunac AD, Krongauz VV and Chang CT, *J Phys Chem* **96**:212 (1992).
- 13 Koch TH and Jones AH, *J Am Chem Soc* **92**:7503 (1970).
- 14 Terrones G and Pearlstein AJ, *Macromolecules* **34**:3195 (2001).
- 15 Ivanov V and Decker C, *Polym Int* **50**:113 (2001).
- 16 Miller G, Gou I, Narayanan V and Scranton AJ, *J Polym Sci A: Polym Chem* **40**:793 (2002).
- 17 Cabral JT and Douglas JF, *Polymer* **46**:4230 (2005).
- 18 Kenning NS, Ficek BA, Hoppe CC and Scranton A, *Polym Int* **57**:1134 (2008).
- 19 Kenning NS, Kriks D, El-Maazawi M and Scranton A, *Polym Int* **55**:995 (2006).
- 20 Rabek JF, *Experimental Methods in Photochemistry and Photophysics*, Part 2. Wiley Interscience, New York (1982).
- 21 Stansbury J and Dickens S, *Dent Mater* **17**:71 (2001).
- 22 Odian G, *Principles of Polymerization*, 3rd edition. Wiley, New York, pp. 222–229 (1991).
- 23 Asmussen S, Arenas D, Cook WD and Vallo CI, *Eur Polym J* **45**:515 (2009).
- 24 Asmussen S, Arenas D, Cook WD and Vallo CI, *Dent Mater* **25**:1603 (2009).
- 25 O'Brien AK and Bowman CN, *Macromolecules* **39**:2501 (2006).
- 26 Tao Y, Yang J, Zeng Z, Cui Y and Chen Y, *Polym Int* **55**:418 (2006).
- 27 Hayki N, Lecamp L, Desilles N and Lebaudy P, *Macromolecules* **43**:177 (2010).